Fabrication of three-dimensional helical microchannels with arbitrary length and uniform diameter inside fused silica

Shengguan He,[1] Feng Chen,[1,*] Keyin Liu,[1] Qing Yang,[1,2] Hewei Liu,[1] Hao Bian,[1] Xiangwei Meng,[1] Chao Shan,[1] Jinhai Si,[1] Yulong Zhao,[1] and Xun Hou[1]

[1]*State Key Laboratory for Manufacturing Systems Engineering & Key Laboratory of Photonics Technology for Information of Shaanxi Province, School of Electronics & Information Engineering, Xi'an Jiaotong University, Xi'an 710049, China*

[2]*e-mail: yangqing@mail.xjtu.edu.cn*

**Corresponding author: chenfeng@mail.xjtu.edu.cn*

Received June 27, 2012; revised August 8, 2012; accepted August 8, 2012; posted August 8, 2012 (Doc. ID 171435); published September 11, 2012

We demonstrate an improved femtosecond laser irradiation followed by chemical etching process to create complex three-dimensional (3D) microchannels with arbitrary length and uniform diameter inside fused silica. A segmented chemical etching method of introducing extra access ports and a secondary power compensation is presented, which enables the fabrication of uniform 3D helical microchannels with length of 1.140 cm and aspect-ratio of 522. Based on this method, a micromixer which consists of a long helical microchannel and a *y*-tape microchannel was created inside the fused silica. We measured the mixing properties of the micromixer by injecting the phenolphthalein and NaOH solution through the two inlets of the *y*-tape microchannel. A rapid and efficient mixing was achieved in the 3D micromixer at a low Reynolds number.

OCIS codes: 140.3390, 140.3330.

Microfluidics has an impressive number of applications in chemical analysis and biomedicine [1,2]. Served as the key parts of the microfluidic devices [3,4], microchannels are commonly fabricated by the conventional photolithography and chemical etching process [5]. The planar or semi-three-dimensional (3D) structures of the microchannels have limited the fluidic performances of the devices.

Generating true 3D microchannels inside transparent materials with a femtosecond (fs) laser allows the creation of high quality microfluidics. Two types of fs laser micromachining techniques have been used for fabricating the embedded 3D microchannels. The first approach is based on ablation-induced removal of materials. The hollow microstructures can be directly photoetched by tightly focused laser pulses. However, when fabricating long and narrow microchannels, debris created by the laser ablation would accumulate inside the structures and block the channels. Even with liquid-assisted ablation processes, the debris problem still exists. Thus, the total length of the microchannels is limited [6–8]. Recently, a kind of porous glass was adopted for the fs laser ablation of 3D microchannels [9,10]. Because pores around the laser scanning path would give space to the debris ejections, the porous glass enabled the generation of complex channels with arbitrary length. However, such a process requires expensive materials and needs a post-annealing process to remove the pores.

Femtosecond laser irradiation followed by chemical etching process (FLICE) is the other approach for producing channels inside transparent materials [11–16]. This method was widely used in photosensitive glasses. Its ablation-free features eliminated the problem of debris. However, when FLICE was used in fused silica (the ideal material for microfluidic applications), the fused silica's very high optical transparency, low background fluorescence, chemical inertness, and hydrophilicity [11] gave rise to the following drawbacks: the length of the fabricated channels is limited to only a few millimeters, and the channels appear as conical shapes with wide entrances and narrow central parts [17,18]. It is a technical challenge to create 3D channels in fused silica with long length and uniform diameter for practical microfluidic applications. In this Letter, we propose an improved FLICE process by introducing extra access ports and laser power compensation. Based on this method, a long 3D helical channel with an aspect ratio of 522 and uniform diameter was fabricated inside fused silica. We devote ourselves to creating practical microfluidic devices with complex 3D structures and perfect optical properties in the UV range, which can be used as biochemical fluorescence detection devices and biophotonic devices for 3D biomedical analysis and bioassay [18]. Our specific helical channel serves as the mixer in these microfluidic devices. Rapid and efficient mixing of this 3D mixer is achieved with a mixing time less than 16 ms and mixing length about 200 μm at a low Reynolds number (Re) of around 2.

As mentioned above, the normal FLICE process would create conical-shaped channels due to the limitation of etching selectivity between the laser-treated and untreated regions of the fused silica. When the hydrofluoric (HF) acid penetrates deeply into the channels, the entrances of the structure suffer a longer chemical etching than the central part, rendering the conical shape as shown in Fig. 1(b).

To make the etching more uniform, we used a simple but practical approach by importing the acid directly into the central part through a series of extra access ports which connect the sample surface and the internal structures, as shown in Fig. 1(c). In this case, HF acid can directly attack the central part of the structures without passing through the long and narrow channels starting from the side openings [19]. As can be seen in Fig. 1(d), the diameter consistency of the microchannels was effectively improved. This method allows the fabrication of

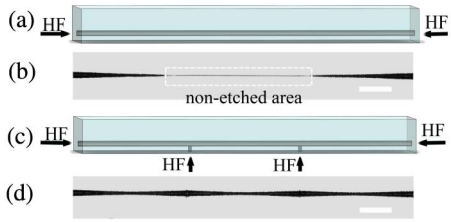

Fig. 1. (Color online) (a) Schematic diagram of the line written inside sample. (b) The optical micrograph of a channel with a non-etched area in its middle. (c) Schematic diagram of microchannels with extra access ports written into the channel. (d) The optical micrograph of a channel with extra access ports. The scale bar represents 300 μm.

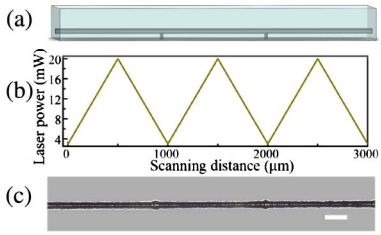

Fig. 3. (Color online) (a) Schematic diagrams of laser-writing line with extra access ports. (b) The laser power curve along the direction of the laser scanning. (c) The optical micrograph of the fabricated uniform channel inside fused silica. The scale bar equals 200 μm.

complex microchannel structures with arbitrary length inside fused silica and glasses. The introduction of the extra access ports enabled the segmented etching of the whole channel, and improved the diameter uniformity of the structures. However, the diameter of the microchannels near the entrances and access ports are still larger than the other parts due to the fact that these regions still suffered relatively longer etching, as shown in Fig. 1(d).

To solve this problem, different levels of laser power were used in the laser scanning process to control the diameters of the microchannels at different sections. First, a series of straight microchannels were created in the fused silica with laser power ranging from 1 mW to 27 mW after a 60-min HF acid etching, as shown in Fig. 2(a). We investigated the power dependency of the diameters of the chemically etched microchannels. The diameters of the fabricated channels were measured and the results were plotted in Fig. 2(b). The results indicate a linear increase of the diameter of the microchannels with the increasing power. Therefore, the differences of the diameters at different sections in the microchannels can be minimized by varying the scanning laser power.

To demonstrate this power compensation method, a long straight microchannel with two extra access ports [Fig. 3(a)] was fabricated by linearly and periodically changing the scanning laser power. Here, the laser power was changed through tuning a computer-controlled attenuator. To decrease the diameter of the channel near the entrances and access ports, the laser power used in these positions was only 3 mW. The laser power was linearly increased to the maximum value of 20 mW when the laser focal spot was approaching the middle points of the two nearby access ports. The relationship between the laser power and the scanning distance is depicted in Fig. 3(b), with the result shown in Fig. 3(c).

Subsequently, a long, complex 3D helical channel was fabricated using the above-described processes. The fabrication process is schematically depicted in Fig. 4. First, a fs laser beam (800 nm, 50 fs, 1 kHz) was focused into the fused silica substrate ($12 \times 12 \times 1.2$ mm^3) by an objective lens with NA = 0.9, and the helical line was written by moving the 3D-stage which carried the sample along the pattern path at a speed of 10 μm /s. During the laser scanning process, the laser power was modulated by a computer-controlled attenuator to implement the power compensation. The height, pitch, and circle diameter of the helical channel can all be controlled by the computer program. After the laser writing process, the sample was etched in 10% HF solution. Finally, a polydimethylsiloxane (PDMS) film was formed on the surface of sample to seal the extra access ports.

In the fabrication process, the extra access ports were introduced at every turn of the helical line. The laser power was changed linearly and periodically from 1 mW to 11 mW. The PDMS seal was formed at room temperature with a very good airtightness level.

A uniform helical microchannel with length about 1.14 cm was obtained after a 1 h etching. The top view of the helical microchannel is shown in Fig. 5(a) with the extra access ports below it. For the helical microchannel, the number of turns, length, screw-pitch, the diameter of circle, and the depth of the helix axis with respect to the sample surface are 30, 2100, 70, 120, and 130 μm,

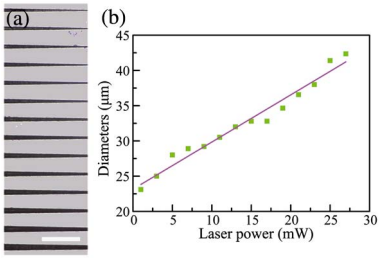

Fig. 2. (Color online) (a) Optical micrograph of channels fabricated under different laser power. The scale bar equals represents 200 μm. (b) Dependence of the diameters of left entrances in channels on the scanning laser power.

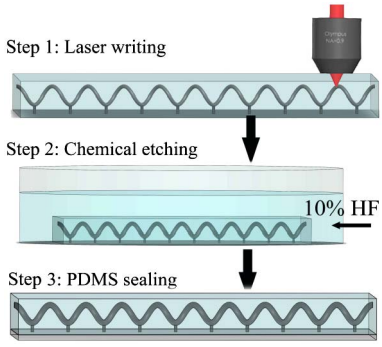

Fig. 4. (Color online) Schematic diagrams of the fabrication process. First, the femtosecond laser writes inside the fused silica. Then, the sample is etched in HF solution. Finally, the PDMS seals the extra access ports.

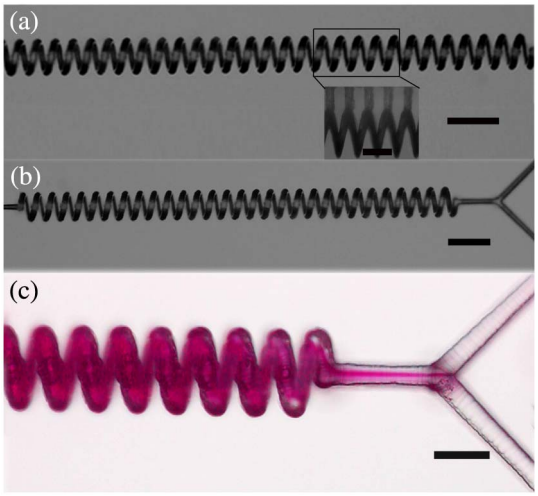

Fig. 5. (Color online) (a) Optical micrograph of a helical channel. The scale bar represents 200 μm. Inset: the side view of the channel (the scale bar is 100 μm). (b) The optical micrograph of the helical micromixer fabricated inside fused silica. The scale bar equals 200 μm. (c) The optical micrograph of microfluidic mixing experiment at Re ≈ 2. The scale bar equals 100 μm.

respectively. The diameter of the cross-section is 20 ± 2 μm and the aspect ratio of the channel is up to 522. Then, a 3D micromixer which consists of the helical microchannel and a y-tape microchannel was designed and fabricated by this method, as shown in Fig. 5(b). The phenolphthalein (the concentration is 0.05 M) and NaOH solution (the concentration is 0.5 M) were injected into the mixer from the right two entrances by a syringe pump with a speed of 0.1 mL/h simultaneously (phenolphthalein becomes pink once mixed with a basic NaOH solution), corresponding to a flow rate of 8.3 cm/s and a low Reynolds number Re ≈ 2. Figure 5(c) shows the mixing performance.

We obtained the color intensity from the captured images pixel by pixel and normalized the intensity. The normalized pixel intensity was calculated as $I_{\mathrm{ni}} = 1 - (I_i - I_{\mathrm{mix}})/(I_{\mathrm{unmix}} - I_{\mathrm{mix}})$, where I_{ni} is the normalized pixel intensity, I_i is the pixel intensity, I_{unmix} is the intensity at the unmixed region, and I_{mix} is the intensity at the fully mixed region. The normalized pixel intensity indicates the degree of mixing for each pixel: 0 means "unmixed" while 1 means "fully mixed." The normalized pixel intensity is as low as 0.3 in the upstream of the straight channel. A sharp increase of mixing index occurs at the joint between the straight channel and helical channel where the chaotic flow arises. The full mixing (the normalized pixel intensity = 1) can be realized after the mixed solution passes through three turns of the helical microchannel (200 μm long) with a mixing time less than 16 ms.

In summary, a uniform 3D helical microchannel with length more than 1 cm and aspect ratio up to 522 was fabricated inside fused silica by an improved FLICE process. The introduction of the extra access ports followed by a power compensation process was adopted to extend the channel length and improve the channel uniformity. A 3D helical micromixer based on the helical channel was demonstrated, and efficient mixing was achieved in the mixer with a mixing time less than 16 ms and mixing length about 200 μm at low Reynolds number (Re ≈ 2). The work provides a method to fabricate 3D channels with arbitrary length and uniform diameter inside fused silica, based on which novel integrated 3D microfluidic devices, such as biochemical fluorescence detection devices and biophotonic devices, can be designed and developed to take advantage of fused silica.

This work is supported by the National Science Foundation of China under the Grant No. 61176113, and the Fundamental Research Funds for the Central Universities.

References

1. G. M. Whitesides, Nature **442**, 368 (2006).
2. A. J. DeMello, Nature **442**, 394 (2006).
3. A. P. Sudarsan and V. M. Ugaz, LAB On Chip **6**, 74 (2006).
4. A. A. S. Bhagat, S. S. Kuntaegowdanahalli, and I. Papautsky, LAB On Chip **8**, 1906 (2008).
5. M. J. Madou, *Fundamentals of Microfabrication: The Science of Miniaturization* (CRC, 2002).
6. Y. Li, K. Itoh, W. Watanabe, K. Yamada, D. Kuroda, J. Nishii, and Y. Jiang, Opt. Lett. **26**, 1912 (2001).
7. C. Li, T. Chen, J. Si, F. Chen, X. Shi, and X. Hou, J. Micromech. Microeng. **19**, 125007 (2009).
8. Y. Li and S. Qu, Opt. Lett. **36**, 4236 (2011).
9. Y. Liao, Y. Ju, L. Zhang, F. He, Q. Zhang, Y. Shen, D. Chen, Y. Cheng, Z. Xu, K. Sugioka, and K. Midorikawa, Opt. Lett. **35**, 3225 (2010).
10. Y. Liao, J. Song, E. Li, Y. Luo, Y. Shen, D. Chen, Y. Chen, Z. Xu, K. Sugioka, and K. Midorikava, LAB On Chip **12**, 746 (2012).
11. R. Osellame, H. J. W. M. Hoekstra, G. Cerullo, and M. Pollnau, Laser Photon. Rev. **5**, 442 (2011).
12. K. C. Vishnubhatla, N. Bellini, R. Ramponi, G. Cerullo, and R. Osellame, Opt. Express **17**, 8685 (2009).
13. F. He, Y. Cheng, Z. Xu, Y. Liao, J. Xu, H. Sun, C. Wang, Z. Zhou, K. Sogioka, K. Midorikawa, Y. Xu, and X. Chen, Opt. Lett **35**, 282 (2010).
14. A. M. Ius, S. Juodkazis, M. Watanabe, M. Miwa, S. Matsuo, H. Misawa, and J. Nishii, Opt. Lett. **26**, 277 (2001).
15. Y. Bellouard, A. Said, M. Dugan, and P. Bado, Opt. Express **12**, 2120 (2004).
16. Y. Cheng, K. Sugioka, K. Midorikawa, M. Masuda, K. Toyoda, M. Kawachi, and K. Shihoyama, Opt. Lett. **28**, 55 (2003).
17. V. Maselli, R. Osellame, G. Cerullo, R. Ramponi, P. Laporta, L. Magagnin, and P. L. Cavallotti, Appl. Phys. Lett. **88**, 191107 (2006).
18. R. Osellame, V. Maselli, R. M. Vazquez, R. Ramponi, and G. Cerullo, Appl. Phys. Lett. **90**, 231118 (2007).
19. V. Maselli, J. R. Grenier, S. Ho, and P. R. Herman, Opt. Express **17**, 11719 (2009).